Anal. Chem. **2002,** *74,* 1972−1978

Disk-Generation/Ring-Collection Scanning Electrochemical Microscopy: Theory and Application

Peter Liljeroth, Christoffer Johans, Christopher J. Slevin, Bernadette M. Quinn,* and Kyösti Kontturi

Laboratory of Physical Chemistry and Electrochemistry, Helsinki University of Technology, P.O. Box 6100, FIN-02015 HUT, Finland.

The potential of ring−disk ultramicroelectrodes (RD UMEs) as probes for scanning electrochemical microscopy (SECM) was investigated both theoretically and experimentally. In particular, the disk-generation/ring-collection (DG/RC) mode of operation was considered. In this case, the interaction of two species with the substrate under investigation can be followed simultaneously from single tip current−distance measurement (approach curve) to the substrate. Theoretical approach curves for DG/RC were calculated by numerical methods. Such approach curves to both insulating and conducting substrates indicate a strong tip response dependence on the ring radius while the response was relatively insensitive to ring thickness and overall tip radius. The RD tip was characterized by fitting experimental approach curves recorded at insulating and conducting substrates to simulated curves for a given tip geometry. DG/RC SECM was then applied to investigate the partitioning of iodine across a liquid−liquid interface.

Scanning electrochemical microscopy (SECM)[1−6] has been used to study charge-transfer phenomena at a wide variety of interfaces, such as polymer films on electrodes,[7] Langmuir monolayers at air−water interfaces,[8−10] phospholipid bilayers,[11,12] and liquid−liquid interfaces,[13−21] in addition to the traditional metal electrode−electrolyte solution interface. One very active area of recent development has been probing spontaneous reactions, such as partitioning at soft interfaces,[14,18,21] adsorption/desorption processes,[22] and dissolution reactions.[23−26] This has been achieved either by equilibrium perturbation (EP)[5,15,22,25,26] or by double potential step chronoamperometry (DPSC−SECM) experiments wherein the species involved in the spontaneous reaction is first generated at the tip, and subsequently, the unreacted amount is probed by a reverse potential step.[5,14,21] Recently, Unwin et al. introduced a triple potential step technique to probe lateral diffusion in electroactive Langmuir monolayers.[27]

We previously reported the use of a ring−disk (RD) microelectrode as a scanning electrochemical microscopy probe.[28] This approach makes it possible to simultaneously monitor two species with a steady-state measurement, thus eliminating the problems associated with double layer charging and, additionally, simplifying the theoretical treatment. The common mode of operation is the disk-generation/ring-collection (DG/RC) in which a redox mediator reacts under diffusion-controlled conditions at the disk and is regenerated at the ring electrode. Conceptually, this mode of operation resembles the DPSC−SECM, wherein a precursor is electrolyzed at the tip during the forward potential step, and then, subsequently, the electrode-generated species is collected during a reverse potential step. As the DG/RC mode of operation

* Corresponding author. Tel: +358 9 451 2572. Fax.: +358 9 451 2580. E-mail: bquinn@cc.hut.fi.

(1) Bard, A. J.; Fan, F. R. F.; Kwak, J.; Lev, O. *Anal. Chem.* **1989**, *61*, 132−138.
(2) Bard, A. J.; Fan, F. R. F.; Pierce, D. T.; Unwin, P. R.; Wipf, D. O.; Zhou, F. *Science* **1991**, *254*, 68−74.
(3) Bard, A. J.; Fan, F. R. F.; Mirkin, M. V. In *Electroanalytical Chemistry*; Bard, A. J., Ed.; Marcel Dekker: New York, 1994; Vol. 18, pp 243−373.
(4) Mirkin, M. V. *Anal. Chem.* **1996**, *68*, 177A−182A.
(5) Unwin, P. R. *J. Chem. Soc., Faraday Trans.* **1998**, *94*, 3183−3195.
(6) Nagy, G.; Nagy, L. Fresenius, J. *Anal. Chem.* **2000**, *366*, 735−744.
(7) Mirkin, M. V.; Fan, F. R. F.; Bard, A. J. *Science* **1992**, *257*, 364−366.
(8) Slevin, C. J.; Ryley, S.; Walton, D. J.; Unwin, P. R. *Langmuir* **1998**, *14*, 5331−5334.
(9) Slevin, C. J.; Unwin, P. R. *J. Am. Chem. Soc.* **2000**, *122*, 2597−2602.
(10) Quinn, B. M.; Prieto, I.; Haram, S. K.; Bard, A. J. *J. Phys. Chem. B* **2001**, *105*, 7474−7476.
(11) Tsionsky, M.; Zhou, J.; Amemiya, S.; Fan, F.-R. F.; Bard, A. J.; Dryfe, R. A. W. *Anal. Chem.* **1999**, *71*, 4300−4305.
(12) Amemiya, S.; Ding, Z.; Zhou, J.; Bard, A. J. *J. Electroanal. Chem.* **2000**, *483*, 7−17.
(13) Slevin, C. J.; Umbers, J. A.; Atherton, J. H.; Unwin, P. R. *J. Chem. Soc., Faraday Trans.* **1996**, *92*, 5177−5180.
(14) Slevin, C. J.; Macpherson, J. V.; Unwin, P. R. *J. Phys. Chem. B* **1997**, *101*, 10851−10859.
(15) Barker, A. L.; Macpherson, J. V.; Slevin, C. J.; Unwin, P. R. *J. Phys. Chem. B* **1998**, *102*, 1586−1598.
(16) Barker, A. L.; Unwin, P. R.; Amemiya, S.; Zhou, J.; Bard, A. J. *J. Phys. Chem. B* **1999**, *103*, 7260−7269.
(17) Barker, A. L.; Slevin, C. J.; Unwin, P. R.; Zhang, J. In *Liquid Interfaces in Chemical, Biological, and Pharmaceutical Applications*; Volkov, A. G., Ed.; Marcel Dekker: New York, 2001; Vol. 95, pp 283−324.
(18) Selzer, Y.; Mandler, D. *J. Phys. Chem. B* **2000**, *104*, 4903−4910.
(19) Kanoufi, F.; Cannes, C.; Zu, Y.; Bard, A. J. *J. Phys. Chem. B* **2001**, *105*, 8951−8962.
(20) Ding, Z.; Quinn, B. M.; Bard, A. J. *J. Phys. Chem. B* **2001**, *105*, 6367−6374.
(21) Barker, A. L.; Unwin, P. R. *J. Phys. Chem. B* **2001**, *105*, 12019−12031.
(22) Unwin, P. R.; Bard, A. J. *J. Phys. Chem.* **1992**, *96*, 5035−5045.
(23) Macpherson, J. V.; Unwin, P. R. *J. Phys. Chem.* **1994**, *98*, 1704−1713.
(24) Macpherson, J. V.; Unwin, P. R. *J. Phys. Chem.* **1995**, *99*, 3338−3351.
(25) Macpherson, J. V.; Unwin, P. R. *J. Phys. Chem.* **1996**, *100*, 19475−19483.
(26) Macpherson, J. V.; Unwin, P. R.; Hillier, A. C.; Bard, A. J. *J. Am. Chem. Soc.* **1996**, *118*, 6445−6452.
(27) Zhang, J.; Slevin, C. J.; Morton, C.; Scott, P.; Walton, D. J.; Unwin, P. R. *J. Phys. Chem. B* **2001**, *105*, 11120−11130.
(28) Liljeroth, P.; Johans, C.; Slevin, C. J.; Quinn, B. M.; Kontturi, K. *Electrochem. Commun.* **2002**, *4*, 67−71.

10.1021/ac015720i CCC: $22.00
Published on Web 03/28/2002

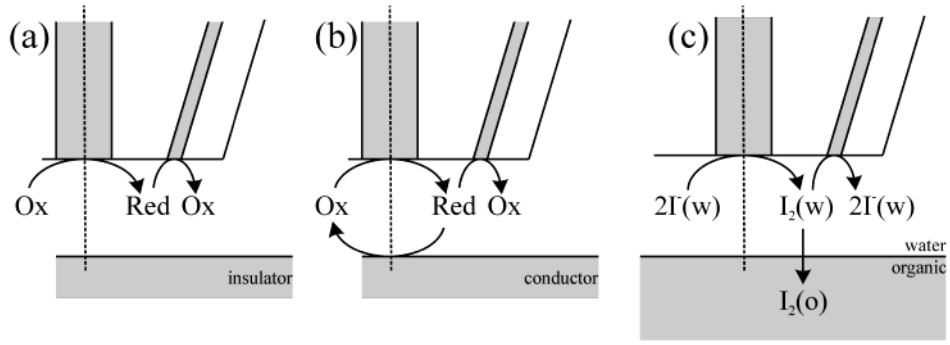

Figure 1. Schematic presentation of the processes studied in this work: (a) an insulating substrate where no reaction occurs, (b) a conducting substrate where the redox mediator is regenerated at the diffusion-controlled rate, and (c) a liquid−liquid interface through which the products of the disk reaction transfer irreversibly.

follows the steady-state response of the electrodes, the time resolution of the instrument used is not as critical as for DPSC−SECM. Very recently, Ufheil et al. proposed ultramicroheptodes as SECM tips wherein the "ring" is formed by six ultramicroelectrodes located on a circle around the middle disk electrode.[29] They presented experimental data for both disk-generation/"ring"-collection and "ring"-generation/disk-collection experiments; however, no theory was presented for the generation−collection experiments.

The manufacture of ring−disk ultramicroelectrodes (RD-UME) by chemical vapor deposition (CVD) was reported previously.[30] Ring ultramicroelectrode SECM tips were prepared by either brushing a glass capillary with Pt paint and subsequent curing or vapor deposition of a gold film onto a pulled optical fiber where the insulating layer has been typically electrophoretic paint.[31−33] Here, the RD tips suitable for SECM measurements were prepared by simply sputtering a gold film onto a normal disk SECM tip, applying an insulating varnish, and subsequent polishing to expose the ring−disk electrode. While the resulting RD is not ideal in terms of perfect concentricity of the electrodes, this simple construction method was demonstrated to provide adequate tips for SECM.

We report here a full theoretical characterization of the DG/RC mode of RD-SECM, as well as the experimental verification for the limiting cases of perfectly insulating (Figure 1a) and conducting substrates (Figure 1b). Finally, the potential of RD-SECM is illustrated by following the partition of iodine across a liquid−liquid interface (Figure 1c).

THEORY OF RD-SECM

The mass transport characteristics of SECM have been theoretically characterized for a number of different experimental conditions and geometries.[3,15,34−38] This section provides the theory

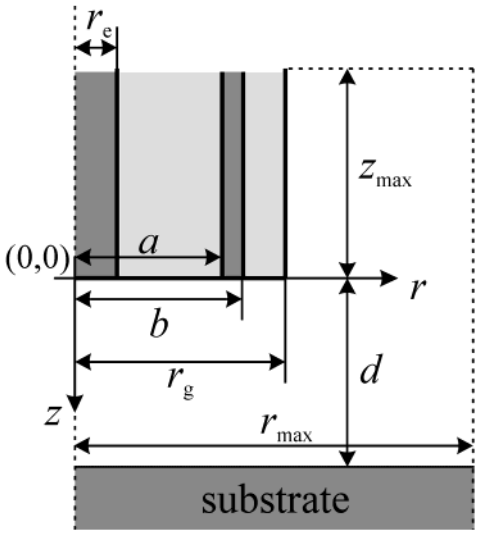

Figure 2. Definition of the coordinate system and the symbols used in this report.

for DG/RC experiments with RD-SECM probes. The reaction under study is a simple n-electron transfer

$$\mathrm{Ox} + ne^- \rightleftarrows \mathrm{Red} \qquad (1)$$

where a redox mediator, Ox, initially present in solution at a concentration of c^b reacts at the disk electrode to form Red initially at zero concentration. Red further reacts at the ring electrode to regenerate Ox. Both electrodes operate under diffusion-limited conditions. The geometry of the ring−disk electrode with relevant symbols is shown in Figure 2. The steady-state problem at hand requires numerical solution of the diffusion equation in cylindrical symmetry, which in dimensionless form is

$$\frac{\partial^2 C(R,Z)}{\partial R^2} + \frac{1}{R}\frac{\partial C(R,Z)}{\partial R} + \frac{\partial^2 C(R,Z)}{\partial Z^2} = 0 \qquad (2)$$

where $C = c/c^b$, $R = r/r_e$, $Z = z/r_e$, and r_e is the radius of the disk electrode. The boundary conditions at the disk and ring electrodes

(29) Ufheil, J.; Borgwarth, K.; Heinze, J. *Anal. Chem.* **2002**, *74*, 1316−1321.
(30) Zhao, G.; Giolando, D. M.; Kirchhoff, J. R. *Anal. Chem.* **1995**, *67*, 1491−1495.
(31) Macpherson, J. V.; Unwin, P. R. *Anal. Chem.* **1998**, *70*, 2914−2921.
(32) Macpherson, J. V.; Jones, C. E.; Unwin, P. R. *J. Phys. Chem. B* **1998**, *102*, 9891−9897.
(33) Lee, Y.; Amemiya, S.; Bard, A. *J. Anal. Chem.* **2001**, *73*, 2261−2267.
(34) Bard, A. J.; Faulkner, L. R. *Electrochemical Methods, Fundamentals and Applications*, 2nd ed.; John Wiley & Sons: New York, 2001.
(35) Mirkin, M. V.; Horrocks, B. R. *Anal. Chim. Acta* **2000**, *406*, 119−146.
(36) Amphlett, J. L.; Denuault, G. *J. Phys. Chem. B* **1998**, *102*, 9946−9951.
(37) Fulian, Q.; Fisher, A. C.; Denuault, G. *J. Phys. Chem. B* **1999**, *103*, 4387−4392.
(38) Fulian, Q.; Fisher, A. C.; Denuault, G. *J. Phys. Chem. B* **1999**, *103*, 4393−4398.

operating under mass transport limited conditions are

$$C(R, Z) = 0; \quad 0 \le R \le 1; \quad Z = 0 \tag{3a}$$

$$C(R, Z) = 1; \quad A \le R \le B; \quad Z = 0 \tag{3b}$$

A no-flux boundary condition is applicable at the insulating material around the tip

$$\partial C/\partial Z = 0; \quad 1 < R < A; \quad Z = 0 \tag{4a}$$

$$\partial C/\partial Z = 0; \quad B < R \le R_G; \quad Z = 0 \tag{4b}$$

$$\partial C/\partial R = 0; \quad R = R_G; \quad -Z_{max} \le Z \le 0 \tag{4c}$$

where $A = a/r_e$, $B = b/r_e$, $R_G = r_g/r_e$, and $Z_{max} = z_{max}/r_e$. Far from the electrodes, the concentration reaches the bulk concentration

$$C(R, Z) = 1; \quad R_G \le R \le R_{max}; \quad Z = -Z_{max} \tag{5a}$$

$$C(R, Z) = 1; \quad R = R_{max}; \quad -Z_{max} \le Z \le L \tag{5b}$$

where $R_{max} = r_{max}/r_e$ and $L = d/r_e$. The boundary conditions for insulating and conducting substrates are, respectively,

$$\partial C/\partial Z = 0; \quad 0 \le R \le R_{max}; \quad Z = L \tag{6a}$$

$$C(R, Z) = 1; \quad 0 \le R \le R_{max}; \quad Z = L \tag{6b}$$

The axis of symmetry has also a no-flux condition

$$\partial C/\partial Z = 0; \quad R = 0; \quad 0 \le Z \le L \tag{7}$$

The problem was solved numerically with Matlab 5.3 equipped with the FEMLAB 1.0 toolbox for solving partial differential equations with the finite element method. The disk (I_{disk}) and ring (I_{ring}) currents were calculated from

$$I_{disk} = 2\pi nFDc^b r_e \int_0^1 R' \frac{\partial C(R', Z)}{\partial Z}|_{Z=0}\, dR' \tag{8}$$

$$I_{ring} = -2\pi nFDc^b r_e \int_A^B R' \frac{\partial C(R', Z)}{\partial Z}|_{Z=0}\, dR' \tag{9}$$

where F is the Faraday constant and D is the diffusion coefficient of the species initially present. The disk and ring currents were normalized with respect to the corresponding diffusion-limited current at distances far from the substrate under study. As was discussed by Galceran et al.,[39] the normalization should be done with respect to an electrode with finite r_g in the bulk solution rather than $4nFDc^b r_e$ applicable for an electrode with infinite r_g. This normalization reduces the effects of the thickness of the ring electrode and the r_g as will be shown later. In the simulations, values of $R_{max} = Z_{max} = 50$ were used. The finite element mesh was refined adaptively until convergence of the calculated current was achieved. The final number of elements was typically of the order of 2×10^5.

EXPERIMENTAL SECTION

Preparation of Electrodes. Disk-shaped Pt SECM probes were prepared as previously described.[3] Briefly, Pt wire (10 and 25 μm, Goodfellows) was heat-sealed in pulled borosilicate glass capillaries (Harvard GC200-10) under vacuum followed by tip sharpening and polishing until the desired ratio of the overall tip diameter to that of the platinum disk was achieved. A thin gold film was subsequently sputtered (Balzers Union SCD 040, sputtering current 30 mA, sputtering distance 30 mm, sputtering time 5 min) onto a continuously rotated tip, and electrical connections were made both to the disk and to the gold film. With the sputtering parameters used, the thickness of the ring electrode was typically of the order of 500 nm as determined by cyclic voltammetry. The probe was then covered with an insulating material, a commercial "nail polish", applied to the tip with a small brush by hand and allowed to dry in air at room temperature. The tip was carefully polished with 0.3-μm aluminum oxide grinding paper (Buehler) until a ring−disk electrode assembly was exposed. This grinding paper was found to be ideal in maintaining a good seal around the ring electrode. As the tip sharpening was done by hand, absolutely uniform shape and perfect concentricity of the disk and ring was not achieved. However, as will be shown in Results and Discussion, the tips proved to be adequate for electrochemical studies.

Chemicals. Hexaammineruthenium chloride ($Ru(NH_3)_6Cl_3$) (Alfa Aesar) and potassium iodide (Riedel-de Haën) were used as the aqueous redox couples. The organic solvent employed in the liquid−liquid partitioning experiments was 1,6-dichlorohexane (1,6-DCHx) (Aldrich). The organic phase was supported in a hydrophobic poly(vinylidene fluoride) (PVDF) membrane (GVHP04700, Millipore Corp.). All other chemicals were of the highest available commercial quality and were used as received. Aqueous solutions were prepared using MQ-treated water (Milli-Q, Millipore Corp.).

Instrumentation. Cyclic voltammograms (CVs) and approach curves (disk and ring current versus distance from the substrate) were measured using a CHI900 SECM instrument (CH-Instruments, Austin, TX). A bipotentiostatic configuration was used where a Pt coil and Ag/AgCl wire served as counter and reference electrodes, respectively, while the ring and disk electrodes were the working electrodes.

RESULTS AND DISCUSSION

The CVs for $Ru(NH_3)_6^{3+}$ reduction obtained separately on both the ring and the disk electrodes are given in Figure 3a. The $Ru(NH_3)_6^{2+}/Ru(NH_3)_6^{3+}$ redox couple is known not to adsorb on metal electrodes, and it has a very high electron-transfer rate constant.[40] Both electrodes show normal steady-state sigmoidal cyclic voltammograms. The diffusion coefficient of $Ru(NH_3)_6^{3+}$ calculated from the limiting current at the disk electrode in a

(39) Galceran, J.; Cecilia, J.; Companys, E.; Salvador, J.; Puy, J. *J. Phys. Chem. B* **2000**, *104*, 7993−8000.

(40) Penner, R. M.; Heben, M. J.; Longin, T. L.; Lewis, N. S. *Science* **1990**, *250*, 1118−1121.

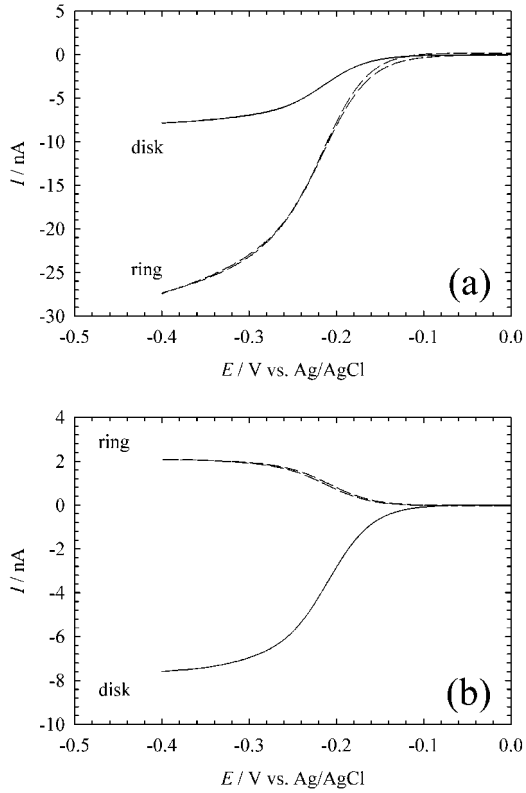

Figure 3. Cyclic voltammograms (a) of 5.1 mM $Ru(NH_3)_6^{3+}$ reduction at the ring (dashed line) and disk (solid line) electrodes in 200 mM LiCl(aq). Sweep rate 10 mV/s. A disk-generation/ring-collection experiment (b). Sweep rate 1 mV/s. Diameter of the disk electrode used was 10 μm.

potential step experiment was $D = 7.2 \times 10^{-6}$ cm^2/s, which compares favorably with the literature.[41,42] The limiting current at a ring embedded in an infinite insulating plane can be calculated from[43]

$$I_{ring} = \frac{nFDc^b\pi^2 b(1 + a/b)}{\ln(16(1 + a/b)/(1 - a/b))} \qquad (10)$$

The ring electrode can be characterized electrochemically by first fitting the measured approach curves to the theoretical ones by varying the ring radius (see below). The thickness of the ring electrode can then be calculated from eq 10. Using the value of the ring radius obtained from the approach curves, $b/r_e = 6$, and the value of the limiting current from a potential step, 25.8 ± 0.2 nA, gives $a/b = 0.9900 \pm 0.0007$; i.e., the thickness of this particular ring electrode is 300 ± 20 nm.

The results of disk-generation/ring-collection voltammetry, where the potential of the disk is scanned and the potential of the ring is kept at a potential where diffusion-limited oxidation of $Ru(NH_3)_6^{2+}$ to $Ru(NH_3)_6^{3+}$ occurs, are given in Figure 3b. The overall collection efficiency is affected by both the radius and the thickness of the ring electrode as well as the overall radius of the tip (r_g). The efficiency is lower than predicted by the theory of Phillips and Stone,[44] who, however, only considered ring−disk electrodes in an infinite insulating plane. A finite r_g will lower the collection efficiency and increase the limiting current.

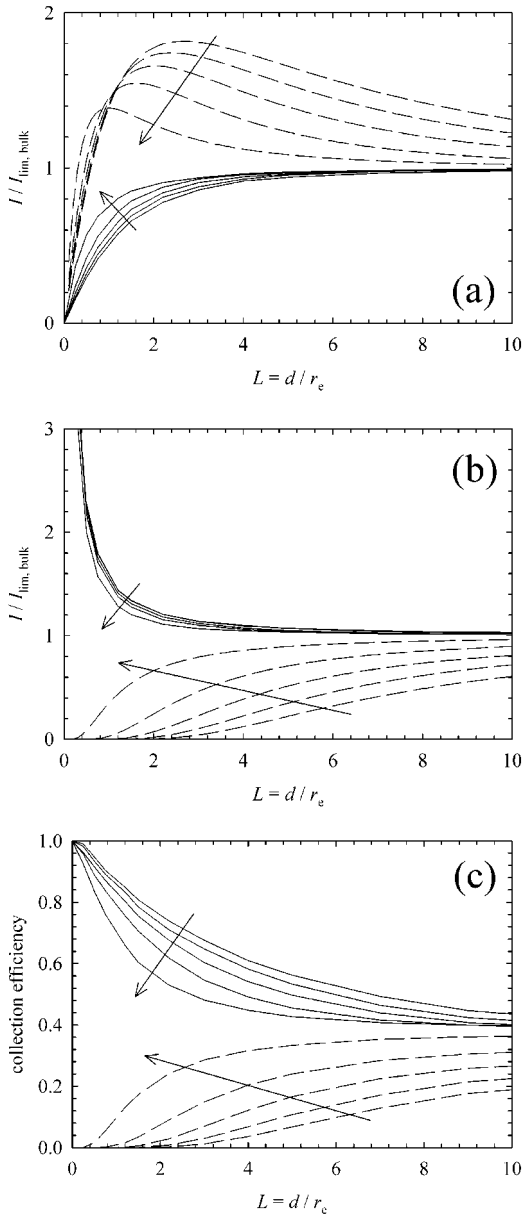

Figure 4. Theoretical approach curves to an insulator (a) and a conductor (b) and the resulting collection efficiency, $|I_{ring}/I_{disk}|$, (c), showing the effect of b/r_e with $B = 2$, 4, 6, 8, and 10 (the arrows point in the direction of decreasing B). Other parameter values employed in the simulations were $a/b = 0.990$, and $R_G = B + 5$.

The dimensionless radius of the ring electrode, $B = b/r_e$, is the main parameter characterizing the RD-SECM tip. Its effect on the normalized disk (solid line) and ring (dashed line) currents versus distance from the substrate for approaches to insulating (a) and conducting (b) substrates are illustrated in Figure 4. The current response at the disk is as expected for a conventional disk SECM tip: negative feedback for an approach to an insulator due to hindered reactant diffusion at the tip and positive feedback for

(41) Daniele, S.; Bragato, C.; Argese, E. *Electrochem. Commun.* **2000**, *2*, 399−403.
(42) Pyo, M.; Bard, A. *J. Electrochim. Acta* **1997**, *42*, 3077−3083.
(43) Szabo, A. *J. Phys. Chem.* **1987**, *91*, 3108−3111.
(44) Phillips, C. G.; Stone, H. A. *J. Electroanal. Chem.* **1997**, *437*, 157−165.

an approach to a conductor due to reactant regeneration.[3] For the collector ring electrode, as the tip approaches an insulator, diffusion of Red away from the disk is blocked by the substrate, and initially, the ring current increases. However, at closer distances, the ring current decreases as the amount of disk-generated Ox is reduced. In contrast, for an approach to a conducting substrate, the concentration changes due to the reaction at the disk are localized in the disk−substrate gap, and thus, the collection current at the ring decreases to zero, as positive feedback at the disk increases. The dimensionless radii used in the calculation were $B = 2$, 4, 6, 8, and 10, the arrow showing the direction of decreasing B. The ring radius determines how far from the substrate the ring current senses the presence of a surface by controlling the extent of the diffusion field generated by the RD assembly. The simulations show that the position of the maximum in the ring current on approaching an insulator is a unique function of the ring radius. The effect of the ring radius on the disk response is qualitatively similar to the effect of r_g in normal SECM.[36] Smaller B makes the response sharper; i.e., changes only occur closer to the substrate. The collection efficiency is shown in Figure 4c for approaches to insulating (solid line) and conducting (dashed line) substrates. For an insulating substrate at sufficiently small tip−substrate separations, the ring collects practically all disk-generated Red and the collection efficiency tends to unity. On the other hand, for a conducting substrate, the redox mediator is regenerated at the substrate rather than at the ring electrode and the collection efficiency tends to zero.

The other variables, in addition to the ring radius, characterizing the ring−disk electrode are the ring thickness (a/b) and the overall diameter of the tip (r_g). The effect of these parameters is negligible for the disk response, as can be seen in Figure 5. As can be seen from Figure 5a, small variations of r_g do not significantly change the ring response for either approach to insulating or conducting substrates. Similarly, variation of the ring thickness does not induce significant change in the ring approach curves, as can be seen in Figure 5b. All of the rings considered in the simulations were thin, i.e., a/b close to 1, consistent with the probes employed in the experiments. It can be concluded that, with the normalization employed here, a ring−disk assembly in SECM experiments is adequately characterized by the ring radius. The ring thickness can be estimated from eq 10 once the radius is known.

Experimental approach curves to both a macroscopic (diameter 3 mm) platinum electrode and PTFE substrate are given in Figure 6. The redox mediator used was $Ru(NH_3)_6^{3+}$ and the disk electrode had a radius of 5 μm. The dotted line is the theoretical fit for $B = 6$, $a/b = 0.990$, and $r_g = 10$. These parameters are consistent with the voltammetric response shown in Figure 3. As expected from previous SECM studies,[34] the approach curve in feedback mode can be modeled with high precision. If a solution containing a trace amount of the redox mediator in the other oxidation state was used (e.g., ferrocenemethanol with a trace amount of ferrociniummethanol), positive feedback at the ring is observed for an approach to a conducting substrate at very short tip−substrate separations (typically, $L < 0.1$; data not shown).

In conventional SECM, the approach speed of the tip to the substrate under investigation must be well below the characteristic

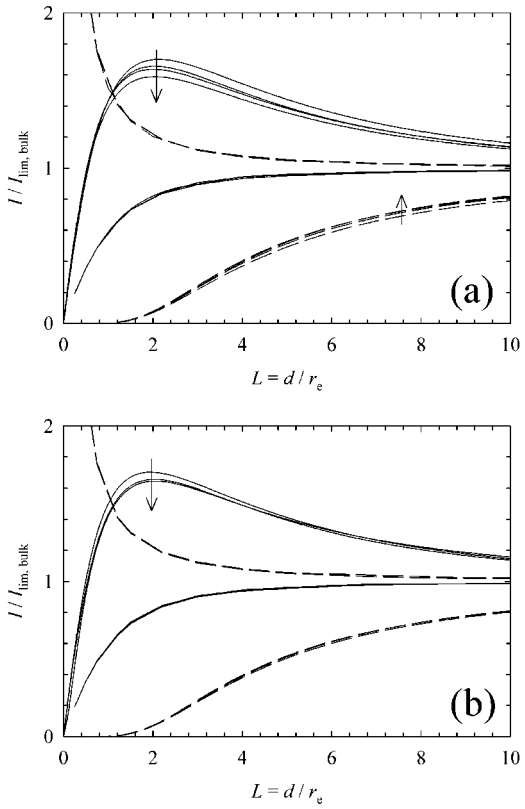

Figure 5. Effect of r_g (a) and a/b (b) on simulated approach curves to an insulating (solid line) and conducting (dashed line) substrates: (a) $a/b = 0.990$, $B = 6$, $R_G = B + 1$, $B + 3$, $B + 5$, and $B + 10$ (arrow shows the direction of decreasing r_g); (b) $B = 6$, $R_G = B + 5$, and $a/b = 0.985$, 0.990, and 0.995 (arrow shows the direction of decreasing a/b).

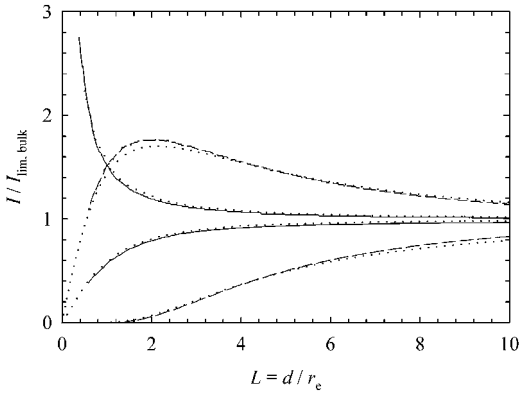

Figure 6. Experimental approach curves for insulating and conducting substrates, disk (solid line) and ring (dashed line) currents in a solution containing 5.1 mM $Ru(NH_3)_6^{3+}$ and 200 mM LiCl. The disk diameter was 10 μm. The disk potential was held at −0.35 V vs Ag/AgCl and the ring 0.0 V vs Ag/AgCl. Approach speed 0.71 (conductor) and 0.18 μm/s (insulator). Dotted lines show the theoretical response with parameter values of $B = 6$, $R_g = B + 10$, and $a/b = 0.990$.

speed of diffusion D/r_e, to obtain steady-state approach curves. In the case of a ring electrode, the characteristic length scale is governed by the ring thickness. However, in the disk-generation/ring-collection mode of SECM operation, the time scale for the ring electrode collector is set by the ring radius, which can easily be 10 times the disk radius with the method used to make the RD-UME used in this study. This means that the collector electrode approaches steady state rather slowly, and correspond-

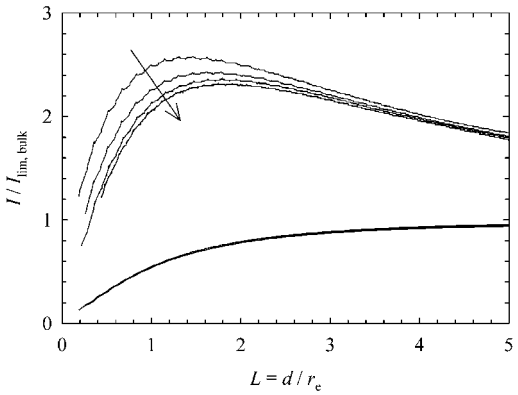

Figure 7. Effect of approach speed on the experimental insulator approach curves for 5.1 mM $Ru(NH_3)_6^{3+}$ in 200 mM LiCl with a 25-μm-diameter disk electrode. Approach speeds were 0.71, 0.36, 0.18, and 0.07 μm/s (the arrow shows the direction of decreasing approach speed). The disk was held at −0.35 V vs Ag/AgCl and the ring at 0.0 V vs Ag/AgCl.

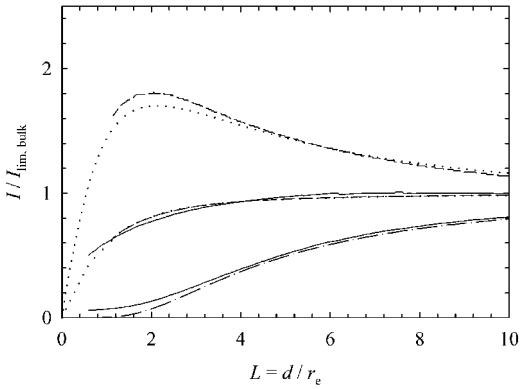

Figure 8. Experimental approach curves to a membrane-supported 1,6-DCHx−water interface. The dashed line shows the response of 1.0 mM $Ru(NH_3)_6^{3+}$ in 200 mM LiCl that does not partition into the organic phase, with the disk biased at −0.35 V vs Ag/AgCl and the ring at 0.0 V vs Ag/AgCl. The solid line is the response from a 1.1 mM iodide solution (200 mM LiCl) with the disk held at 0.6 V vs Ag/AgCl and the ring at 0.0 V vs Ag/AgCl. The disk radius was 5 μm and the approach speed 0.25 μm/s for iodide oxidation and 0.1 μm/s for $Ru(NH_3)_6^{3+}$ reduction. The dotted line shows the theoretical response for an insulating substrate and the dash−dotted line is the theoretical ring response for a conducting substrate, both with $B = 6$, $R_G = B + 5$, and $a/b = 0.990$.

ingly, slow approach speeds must be utilized. This is illustrated in Figure 7, where experimental approach curves to an insulating substrate were obtained at different approach speeds. In this case, the tip employed had a disk radius of 12.5 μm and a ring radius of ∼100 μm (i.e., $B = 8$). To observe a steady-state response, the approach speed with this experimental setup must be lower than 0.07 μm/s, which means that a typical approach curve over a distance of 100 μm would take ∼10 min to measure. The problem is readily circumvented by the use of smaller tips, which first decreases the time required to reach steady state (for the same dimensionless ring radius, this characteristic time scales as the square of the disk diameter) and, second, shortens the distance over which the approach curve needs to be measured. This problem is not as serious for conducting substrates as the regeneration of the redox mediator takes place mostly at the substrate under study and the changes in the ring current are not as rapid as with an insulating substrate. However, it must be stressed that the approach speed does not alter the qualitative features of the ring response.

To assess the potential of the RD-SECM to study spontaneous reactions at interfaces, the partitioning of iodine across a liquid−liquid interface was studied. Approach curves to a water−dichlorohexane interface are given in Figure 8. The organic phase was supported on a PVDF membrane. The solution contained both $Ru(NH_3)_6^{3+}$ and iodide. The dashed line is the approach curve when the tip is held at −0.35 V versus Ag/AgCl and the ring at 0.0 V versus Ag/AgCl corresponding to diffusion-limited generation and collection of $Ru(NH_3)_6^{3+}$ at the disk and ring electrodes, respectively. This redox couple does not react at the interface, and thus, insulating behavior is observed. The dotted line gives the theoretical response to an insulator. The solid line is the response as the tip is held at 0.6 V versus Ag/AgCl and the ring at 0.0 V versus Ag/AgCl corresponding to diffusion-limited generation and collection of iodide at the disk and ring electrodes, respectively, according to the electrode reaction $I^-(aq) + e^- \rightleftarrows {}^1/_2 I_2(aq)$. Formation of solid iodine on the electrode surface occurs when the solubility is exceeded (1.1 mM in water at 25 °C[45]). Also, when the concentration of iodide is sufficiently low, the formation of triiodide according to $I^-(aq) + I_2(aq) \rightleftarrows I_3^-(aq)$ can be neglected. Compton and co-workers showed that, in sulfuric acid solutions, solid iodine is not formed and the formation of triiodide can be neglected, if the concentration of iodide is less than ∼3 mM.[46] Thus, to avoid these complications, a concentration of 1.1 mM KI was used. Cyclic voltammetry showed no evidence of solid iodine formation as the voltammograms did not display a distinctive kink described in ref 46. Qualitatively, the RD-SECM response of iodide at a liquid−liquid interface can be rationalized as follows: iodide does not partition into the organic phase and the disk response shows normal negative feedback. On the other hand, the disk-generated iodine readily partitions into the organic phase (partition coefficient of ≫1), and consequently, the ring response resembles the conductor response. The strong partitioning behavior is similar to that found by Slevin et al. for bromine partitioning across a water−1,2-dichloroethane interface.[14] The observed response deviates from the theoretical limiting case at short tip−substrate separations, which is probably due to either (i) kinetic limitations of iodine partitioning or (ii) establishment of a partitioning equilibrium due to a finite value of the partition coefficient. Work is in progress to distinguish between these two cases and to extract parameters characterizing the partitioning (rate constants and partition coefficient).

CONCLUSIONS

We have presented detailed theoretical characterization of DG/RC SECM in conjunction with RD-UMEs. The theoretical results compare favorably with experiments for the limiting cases of perfectly conducting or insulating substrate. To illustrate the potential of RD-SECM for probing reactions at interfaces,

(45) Swathirajan, S.; Bruckenstein, S. *J. Electroanal. Chem. Interfacial Electrochem.* **1980**, *112*, 25−38.

(46) Akkermans, R. P.; Fulian, Q.; Roberts, S. L.; Suarez, M. F.; Compton, R. G. *J. Phys. Chem. B* **1999**, *103*, 8319−8327.

partitioning of iodine across an immiscible liquid−liquid interface was demonstrated. A distinct advantage of RD-SECM in comparison with the DPSC−SECM[14,21] is that low concentrations of the electroactive species can be employed because measurements are carried out in steady state and double layer charging current is absent.

The future work will concentrate, both experimentally and theoretically, on exploring reactions at soft interfaces, which are of interest in, for example, two-phase catalysis. In addition, probing phenomena such as lateral diffusion in monolayers[9,27] should be amenable to investigation by RD-SECM. Experimentally, different insulating materials are being considered in order to be able to use RD-SECM also in organic solvents.

ACKNOWLEDGMENT

The authors gratefully acknowledge Dr. Erkki Heikinheimo for use of the sputtering equipment. Financial support from The Finnish Academy and the National Technology Agency (Finland) is greatly appreciated.

Received for review December 5, 2001. Accepted February 22, 2002.

AC015720l